Computational Analysis of Aeroacoustic Effect of a Seal on Slat Cove for Different Angles of Attack

Fernando H. T. Himeno, fernando.himeno@usp.br
Daniel S. Souza, dss-em@usp.br
Filipe R. do Amaral, framaral@usp.br@usp.br
Marcello A. F. Medeiros, marcello@sc.usp.br

Universidade de São Paulo, São Carlos, São Paulo, Brazil

Abstract: *The work to be presented aims at studying the effect of a seal on the slat cove surface, commonly observed in real scale airplanes,on the turbulent structures inside the cove potentially related to aeroacoustic noise generation. Time-resolved simulations of the flow around an high-lift geometry was computed using the commercial code PowerFLOW, which is based on the Lattice-Boltzmann method. An algorithm based on the Ffowcs Williams-Hawkings analogy was used for noise propagation from near to far field. Comparisons between the present simulations with experimental data processed with beamforming technique allied with a deconvolution method will be made to assess the quality of the numerical solution. Analysis of aeroacoustic seal influence for different angles of attack is proposed. Additionally, analysis of the the effect of the seal on relevant time average flow quantities, instantaneous field and fluctuation spectral contents will be carried out.*
Keywords: *slat, Lattice-Boltzmann, POD*

1. INTRODUCTION

Considerable part of airplane propagated noise is due to engines, landing gear and aerodynamic surfaces. With development of high bypass turbofans, used in commercial airplanes, noise contribution of motors decreased substantially in last decades, increasing airframe contribution percentage in general noise. For this reason, several researches are conducted to study aeroacoustic phenomena related to airframe. Significant part of this noise during approximation maneuvers are due to high-lift devices, slat and flap. Slat noise however, is considered not punctual source since this device is present along almost whole wingspan.(Dobrzynski, 2010; Souza *et al.*, 2015)

Early studies(Jenkins *et al.*, 2004; Dobrzynski, 2010; Imamura *et al.*, 2009) presented a separation in noise spectra due to slat in broadband component, high frequency tones and tonal peaks in low and mid-frequency over broadband noise. Both numerical(Khorrami *et al.*, 2004; Singer *et al.*, 2000) and experimental(Jenkins *et al.*, 2004) works investigated the physics of the high frequency tone and concluded that it was generated by the shedding of discrete vortices in the blunt slat trailing edge. On the other hand, the exact mechanisms responsible for the low frequency tonal peaks and broadband noise, which correspond to the dominant portion of the noise spectrum remains unclear, although it is well accepted that they are related to the turbulent structures developing in the free shear layer separating the low velocity recirculating zone in the slat cove from the accelerated flow between the slat and the main element (Khorrami *et al.*, 2002a,b; Choudhari *et al.*, 2002; Khorrami *et al.*, 2004). Some theories relating the series of low frequency peaks to Rossiter modes in open cavity flows (Roger and Perennes, 2000; Kolb *et al.*, 2007; Terracol *et al.*, 2011).

Real slats have excrescences over its surfaces as deflection mechanisms anti-icing tubes and seals that changes the dynamics of flow and potentially the aeroacoustic response of slat device. The focus of the present efforts is on the effects of a seal at the surface of the slat cove. Two-dimensional Zonal simulations by Khorrami et al.(Khorrami and Lockard, 2010) indicated that such a seal has no significant impact on the slat noise characteristics. In contrast, three-dimensional Lattice-Boltzmann simulations by Bandle et al.(Bandle *et al.*, 2012) and wind tunnel measurements by Amaral et al.(Amaral *et al.*, 2015) showed substantial change in the amplitude and spectral distribution of slat noise as the seal was considered. Additionally, the results by (Bandle *et al.*, 2012) and (Amaral *et al.*, 2015) indicated a considerable sensitiveness of the results regarding the seal position. Three aspects may explain the differences between the Navier-Stokes results and the results from the Lattice-Boltzmann simulations and the wind tunnel experiments: 1. The spatial dimensionality of the problems considered; 2. The nonconformity between the investigations regarding the seal position and; 3. the dependence of the problem on the geometry of the airfoil itself (Bandle et al.'s and Amaral et al.'s studies considered the MD30P30N geometry while Khorrami et al. studied the flow over one section of the 777-'s wing).

Using the Proper Orthogonal Decomposition (POD) technique with provided by unsteady Lattice-Boltzmann computations, Souza et al.(Souza *et al.*, 2015) compared the coherent structures related to a low frequency peak in the spectrum of slat noise for two of the configurations studied by (Bandle *et al.*, 2012), the clean configuration and one with the seal on the cove. The noise spectrum predicted for the configuration with the seal had significantly stronger low frequency peaks than the noise computed for the clean configuration. Their results indicated that the turbulent flow inside the cove with the seal possesses more organized structures oscillating at the peak frequency than the clean cove. Those better organized structures are expected to be more efficient in the generation of aeroacoustic noise. Although the Lattice-Boltzmann computations were three-dimensional, the data processed with POD comprised the signal of only one section of the simulation. Therefore it did not provide any information about the effect of the seal on the spanwise organization of the structures

inside the slat cove, which seem to be of greatest relevance for the understanding of the flow mechanism responsible for the generation of low frequency peaks(Pascioni *et al.*, June 2014; Pagani *et al.*).

Our present effort aims at investigating the effect of the seal located on the surface of the slat cove on the dynamics of the turbulent flow inside the cove of the wind tunnel model tested at the USP wind tunnel facilities at São Carlos(Amaral *et al.*, 2015) by means of unsteady Lattice-Boltzmann simulations. Besides the clean configuration, one of the configurations with the tested in the wind tunnel will be considered, both at two angles of attack. The computational model has been used in previous investigations of the slat noise and showed good comparison with experimental results for the dominant portion of the noise spectrum(Pagani *et al.*). Comparison between the numerical and experimental results of the time average pressure coefficient and far-field noise spectra will be provided.

2. NUMERICAL MODEL

2.1 High-lift Geometry MD30P30N

Simulations presented here uses MD30P30N, a high-lift airfoil widely studied in literature(Jenkins *et al.*, 2004; Khorrami *et al.*, 2004; Bandle *et al.*, 2012; Souza *et al.*, 2015). The airfoil stowed chord (c_{stowed}) were $0.5\ [m]$ and simulated domain span of $0.0512\ [m]$. Slat cusp were considered sharp and trailing edge blunt with thickness of $0.092\% \cdot c_{stowed}$. A square seal is considered on slat geometry (Fig. (1)) with $3\ [mm]$ of dimension, at position of $d = 30\ [mm]$ and the angle of attack analyzed are $3\ [^\circ]$ and $7\ [^\circ]$. The infinite flow velocity were $U_{infty} = 34\ [m/s]$, Mach number of $M = 0.1$ and Reynolds of $Re = 1 \cdot 10^6$. Data acquisition points over the surfaces of slat and main element and the determination of the distance d of seal from trailing edge are represented in Fig. (1).

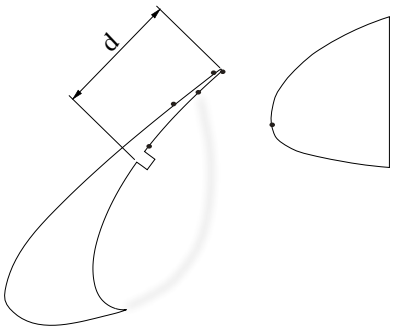

Figure 1: Slat geometry detail with data acquisition points and seal position represented.

2.2 Lattice-Boltzmann Method

Commercial code used in this work were PowerFLOW 5.0 (EXA), software based on Lattice-Boltzmann Method that solves the discrete Boltzmann equation for probability density function:

$$f(\vec{r} + \vec{c}\delta t, \vec{c}, t + \delta t) - f(\vec{r}, \vec{c}, t) = \Omega(f). \tag{1}$$

Function $f(\vec{r}, \vec{c}, t)$ represents the tendency to find a particle at time t in position $\vec{r}$ with velocity $\vec{c}$. The collision term represented by Ω, is related to momentum exchange between particles and were approximated for aeronautical problems by (Bhatnagar *et al.*, 1954) as $\Omega(f) = -\frac{1}{\tau} \cdot (f - f^{eq})$, where τ represent the relaxation time and f^{eq}, the equilibrium probability density function; so we have

$$f(\vec{r} + \vec{c}\delta t, \vec{c}, t + \delta t) - f(\vec{r}, \vec{c}, t) = -\frac{1}{\tau}[f(\vec{r}, \vec{c}, t) - f^{eq}(\vec{r}, \vec{c}, t)]. \tag{2}$$

Mesh performed by PowerFLOW is composed of cubic volumes aligned with the Cartesian coordinates. To represent the effect of the smallest turbulent scales a Renormalization Group k-ϵ turbulence model is used. For analyses of far-field propagated sound, code uses a *Ffowcs Williams-Hawkings* (FW-H) analogy algorithm, based on Farassat's 1A formulation (Bres *et al.*, 2009). Since the *Mach* numbers in present analysis are low, the quadrupole sources in the flow were not taken into account in the FW-H calculations. Therefore, only the slat and the aft portion of the main element surfaces are taken into integration account for near field. For far-field propagated noise in spanwise direction a center region of domain span with length of half total domain were considered in order to avoid the periodicity condition applied on lateral walls.

3. EXPERIMENTAL MODEL

The experiments were run in the closed circuit wind-tunnel of the São Carlos Engineering School. The closed test section of the tunnel was $1.3\ [m]$ high, $1.7\ [m]$ wide and $3.0\ [m]$ long, with a contraction ratio of $1:8$ and is equipped with an axial fan with 8 blades, driven by a 115 [HP] alternated current motor. The tunnel was able to reach velocities up to $34\ [m/s]$. To provide more two-dimensional flow, wall boundary layer control was done by applying suction upstream of the slat and on the suction side of the main element.

The MD30P30N wing model used in the experiments was basically manufactured in aluminum alloy and spanned the entire tunnel height of $1.3\ [m]$ and the airfoil chord at stowed configuration was $0.5\ [m]$. The instrumentation of model included static pressure tapings at the center span along a streamwise direction, distributed on slat, main element and flap. In order to monitor two-dimensionality of the time averaged flow over the model, tapings were positioned along the spanwise direction in two positions at the suction side of the main wing, one positioned near its leading edge and another near its trailing edge.

Aeroacoustic measurements have been performed with an optimized Archimedean spiral array composed of 62 flush-mounted microphones. The array was wall-mounted in a position from which it is possible to focus on the wing model lower surface by a proper signal processing technique. The microphones used are of *GRAS 46BD* $\frac{1}{4}$ in type. The data acquisition systems are based on *National Instruments hardware*. For the pressure measurements, hardware from *Scanivalve Coorporation* were employed, including *ZOC33* scanning modules.

3.1 Beamforming technique with DAMAS

For experimental data post-processing, conventional beamforming technique with *DAMAS* deconvolution method were employed with in-house codes implemented at frequency domain. A scanning plan, containing a discrete mesh of N points, is defined around the assumed noise source region. The beamforming code used here weights the cross-spectral matrix (*CSM* - outer product of sound pressure level spectral estimates), processed from array microphone measurements with steering vectors stemmed from transfer functions that models the sound propagation from each mesh focal point to all array microphones as monopole sources for either frequency. By successively focusing the array pattern to each target point of a scanning grid, it is possible to achieve a spatial pressure level distribution, indicating the most likely source position according to a contour level map known as beamforming map, (Mueller *et al.*, 2002). The conventional beamforming output, following the methodology presented at (Sarradj, 2012), is given by

$$b(\vec{r}_{o,n},\omega) = \mathbf{h}^{\dagger}(\vec{r}_{m,n},\omega)\left\langle \mathbf{p}(\vec{r}_{m,o},\omega)\mathbf{p}^{\dagger}(\vec{r}_{m,o},\omega)\right\rangle \mathbf{h}(\vec{r}_{m,n},\omega) \tag{3}$$

where n is a mesh point to be scanned in searching for noise sources, with $1 \leq n \leq N$, known as focus point; o as the reference position, or origin; m is the $m-th$ microphone position, where $1 \leq m \leq M$ with M being the total number of microphones. In this formulation b is a scalar representing a squared sound pressure estimate at angular frequency ω, on the focus point n (with $\vec{r}_{o,n}$ being the position vector), relative to a reference given by o. $\mathbf{p}$ is a vector that contains the spectral estimate of sound pressure level written as Fourier Transforms of microphones signal at position vector $\vec{r}_{m,o}$. $\mathbf{h}$ is the steering vector, that are normalized transfer functions used to model the propagation of an acoustic wave emitted from a mesh point at position $\vec{r}_{o,n}$ to the microphone m. The symbol $\dagger$ refers to the Hermitian operator, and $\langle\cdots\rangle$ denotes an averaging over the number of data blocks. Both vectors, $\mathbf{p}$ and $\mathbf{h}$, are of $M \times 1$ dimension.

Due to finite spatial sampling and array aperture which lead to limited array resolution and dynamic range, the beamforming map is biased by the array design and not necessarily represent the actual source distribution. This drawback may be greatly remedied by a deconvolution between the measured sound field and the array pattern associated with a modeled distribution of forces. At *DAMAS* deconvolution method, introduced by (Brooks and Humphreys, 2006), the goal is that the desired quantities, such as sound pressure levels and sources distributions, are extracted independently of the array's characteristics. It is assumed N sources statistically independent, each one in a different position at the mesh. A linear system, with N unknowns, is set up in a way to connect conventional beamforming point's field with its equivalent source distribution at the same point's location. The sources distribution is iteratively solved. Thus, the problem can be written as

$$\mathbf{b} = A \cdot \mathbf{X} \tag{4}$$

This linear equation system, relates the space point's field with beamforming given by the array's response, $\mathbf{b}$, of dimension $N \times 1$, and its equivalent sources distribution, $\mathbf{X}$, of dimension $N \times 1$. A is a square matrix of order N, gathering all array point spread functions (*psf*). Since the system in Eq. (4) is highly ill-conditioned, a modified Gauss-Seidel iterative method, considering a positivity constrain to avoid non-physical negative source auto-power estimate, was applied, (Brooks and Humphreys, 2006).

4. PRELIMINARY RESULTS

Pressure coefficient on the airfoil surface, comparing simulation results and experiments are showed in Fig. (2). Good agreement between the numerical and experimental results is observed. For $AoA = 7\ [^{\circ}]$, the level of the main element suction peak is underpredicted by approximately 0.5 on C_p. It is seen, that the simulations predict a premature separation of the boundary layer in to the wind-tunnel experiments. This can be due to poor solution of the boundary by the Lattice-Boltzmann code, which uses wall function to approximate the solution at the volumes closest to the airfoil walls. Nevertheless, this difference does not seem to have significant influence on the slat mean aerodynamics and the agreement between numerical and experimental results for surface static pressure is deemed good for our purposes. It is seen that the seal on the slat cove has little influence on the mean static pressure distribution. For $AoA = 3\ [^{\circ}]$, it slightly increases the level of the main element suction peak.

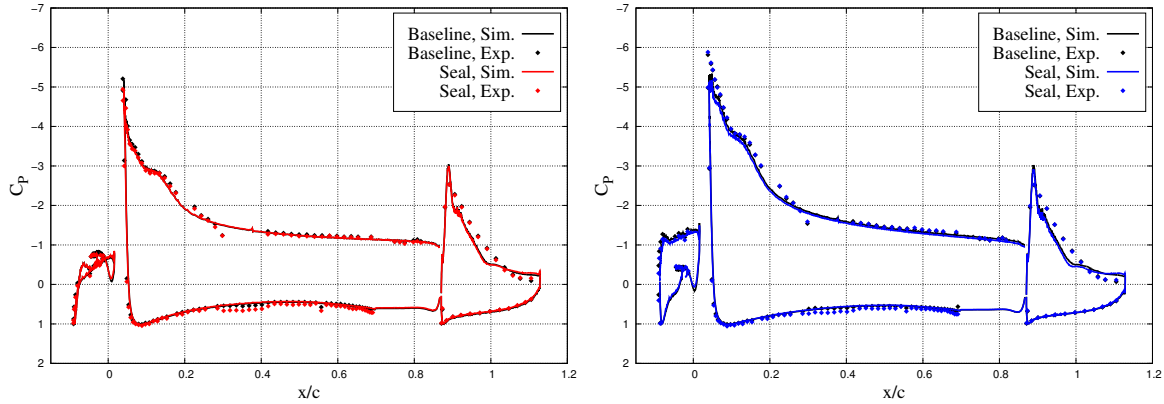

(a) $AoA = 3°$ (b) $AoA = 7°$

Figure 2: Comparison between simulated and experimental cp distribution for baseline and seal cases for $d = 30$ $[mm]$.

The far-field noise propagated from slat region are presented in Fig. (3) for $AoA = 3$ $[°]$ and $AoA = 7$ $[°]$. Again good comparison is observed between numerical and experimental results, mainly for the baseline configuration. A persistent difference between the methodologies is seen for the frequency band between Strouhal 14 and 20. As preliminary studies indicate, it might be caused by insufficient extension of the computational domain in the spanwise direction. However, the noise level at this band is more then 20 dB/Hz below the dominant slat noise and is therefore not the focus of the present study. As observed in previous computational analyzes (Bandle *et al.*, 2012; Souza *et al.*, 2015), the main effect of the seal on the slat noise spectrum is in the dominant series of low-frequency narrowband peaks. As we introduced the seal on the slat cove, the amplitude of some of the peaks increased and their frequencies shifted a little to lower frequencies. This is somewhat different from the computations by (Souza *et al.*, 2015) with higher Reynolds number (1.7 million), for which only the increase of the peak amplitudes were observed as the seal was considered. Considering the wind-tunnel measurements, the peak of lowest frequency was the most affected by the presence of the seal. In comparison to the baseline configuration its measured amplitude is approximately 20 dB/Hz larger in the cases with the seal. The simulations managed to capture the frequency shift of the peaks, but the level enhancement of the first peak was captured only partially.

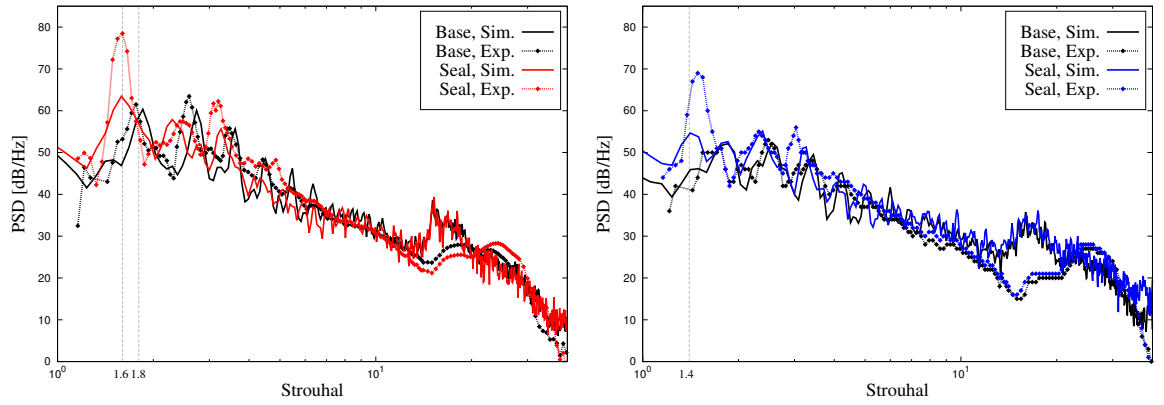

(a) $AoA = 3°$ (b) $AoA = 7°$

Figure 3: Comparison between experimental and simulated propagated noise at array center for baseline and seal cases.

5. FURTHER ANALYSIS

Although the simulations did not predict the same increase in the peak amplitude caused by the seal as in the wind tunnel experiments, the frequency shift of the peaks and part of their amplification were captured. It seems therefore reasonable to use the simulation results to investigate, at a qualitative perspective, the effect of the seal on the characteristics of the turbulent structures inside the cove and their interaction with the airfoil surface. For that, we will analyze the change caused by the seal in time averaged flow quantities, as the streamlines, velocity magnitude and resolved turbulent kinetic energy as well instantaneous field of the spanwise vorticity and λ_2 criterion. Also the spectral content of the fluctuations inside the cove and the level of coherence of these fluctuations in the spanwise direction will be computed.

6. ACKNOWLEDGEMENTS

Fernando H.T. Himeno received support grant $\#2016/02970-5$, São Paulo Research Foundation (FAPESP), Daniel S. Souza and Filipe R. Amaral received funding from CAPES/Brazil - Coordenação de Aperfeiçoamento de Pessoal de

Nível Superior. Marcello A.F. Medeiros Received support from CNPq/Brazil - Conselho Nacional de Desenvolvimento Científico e Tecnológico.

7. REFERENCES

Amaral, Filipe R., S., S., D., Pagani, C.P.J., Himeno, F.H.T. and Medeiros, M.A.F., 2015. "Experimental study of the effect of a small 2d excrescence placed on the slat cove surface of an airfoil on its acoustic noise". *AIAA Aeroacoustics Conference*.

Bandle, L., Souza, D.S., Simoes, L.G. and Medeiros, M.A., 2012. "On detrimental effects of excrescences on the slat noise". *AIAA Aeroacoustics Conference*, Vol. 33.

Bhatnagar, P.L., Gross, E.P. and Krook, M., 1954. "A model for collision processes in gases. i. small amplitude processes in charged and neutral one-component systems". *Physical review*, Vol. 94, No. 3, p. 511.

Bres, G.A., Pérot, F. and Freed, D., 2009. "Properties of the lattice-boltzmann method for acoustics". In *Proc. AIAA Aeroacoustics Conf., Miami, USA*.

Brooks, T.F. and Humphreys, W.M., 2006. "A deconvolution approach for the mapping of acoustic sources (damas) determined from phased microphone arrays". *Journal of Sound and Vibration*, Vol. 294, No. 4-5, pp. 856–879. ISSN 0022-460X. doi:10.1016/j.jsv.2005.12.046. URL `<Go to ISI>://WOS:000238359200011`.

Choudhari, M., Khorrami, M.R., Lockard, D.P., Atkins, H. and Lilley, G., 2002. "Slat cove noise modeling: A posteriori analysis of unsteady rans simulations". *AIAA paper*, Vol. 2468, p. 2002.

Dobrzynski, W., 2010. "Almost 40 years of airframe noise research: what did we achieve?" *Journal of aircraft*, Vol. 47, No. 2, pp. 353–367.

Imamura, T., Ura, H., Yokokawa, Y. and Yamamoto, K., 2009. "A far-field noise and near-field unsteadiness of a simplified high-lift-configuration model (slat)". *AIAA paper*, Vol. 1239, p. 2009.

Jenkins, L.N., Khorrami, M.R. and Choudhari, M., 2004. "Characterization of unsteady flow structures near leading-edge slat: Part i. piv measurements". *AIAA paper*, Vol. 2801, p. 2004.

Khorrami, M.R., Choudhari, M.M. and Jenkins, L.N., 2004. "Characterization of unsteady flow structures near leading-edge slat: Part ii. 2d computations". *AIAA Paper*, Vol. 2802, p. 2004.

Khorrami, M.R. and Lockard, D.P., 2010. "Effects of geometric details on slat noise generation and propagation". *International Journal of aeroacoustics*, Vol. 9, No. 4, pp. 655–678.

Khorrami, M.R., Singer, B.A. and Berkman, M.E., 2002a. "Time-accurate simulations and acoustic analysis of slat free-shear-layer". *AIAA journal*, Vol. 40, No. 7, pp. 1284–1291.

Khorrami, M.R., Singer, B.A. and Lockard, D.P., 2002b. "Time-accurate simulations and acoustic analysis of slat free-shear-layer: Part ii". *AIAA paper*, Vol. 2002-2579.

Kolb, A., Faulhaber, P., Drobietz, R. and Grünewald, M., 2007. "Aeroacoustic wind tunnel measurements on a 2d high-lift configuration". *AIAA paper*, Vol. 3447, p. 2007.

Mueller, T.J., Allen, C.S., Blake, W.K., Dougherty, R.P., Lynch, D., Soderman, P.T. and Underbrink, J.R., 2002. *Aeroacoustic Measurements*. Springer, Berlin.

Pagani, C., Souza, D. and Medeiros, M., ???? "Slat noise: aeroacoustic beamforming in closed-section wind tunnel with numerical comparison". *AIAA Journal*. Accepted for publication.

Pascioni, K., Cattafesta, L. and Choudhari, M., June 2014. "An experimental investigation of the 30P30N multi-element high-lift airfoil". AIAA Paper 2014-3062.

Roger, M. and Perennes, S., 2000. "Low-frequency noise sources in two-dimensional high-lift devices". In *6th Aeroacoustics Conference and Exhibit*. American Institute of Aeronautics and Astronautics, Aeroacoustics Conferences. doi:doi:10.2514/6.2000-1972 10.2514/6.2000-1972. URL `http://dx.doi.org/10.2514/6.2000-1972`. Doi:10.2514/6.2000-1972.

Sarradj, E., 2012. "Three-dimensional acoustic source mapping with different beamforming steering vector formulations". *Advances in Acoustics and Vibration*, Vol. 2012, p. 12. doi:10.1155/2012/292695. URL `http://dx.doi.org/10.1155/2012/292695`.

Singer, B.A., Lockard, D.P. and Brentner, K.S., 2000. "Computational aeroacoustic analysis of slat trailing-edge flow". *AIAA journal*, Vol. 38, No. 9, pp. 1558–1564.

Souza, D., Rodríguez, D., Simões, L. and Medeiros, M., 2015. "Effect of an excrescence in the slat cove: Flow-field, acoustic radiation and coherent structures". *Aerospace Science and Technology*.

Terracol, M., Manoha, E. and Lemoine, B., 2011. "Investigation of the unsteady flow and noise sources generation in a slat cove: hybrid zonal rans/les simulation and dedicated experiment". In *20th AIAA Computational Fluid Dynamics Conference*. American Institute of Aeronautics and Astronautics. doi:doi:10.2514/6.2011-3203. URL `http://dx.doi.org/10.2514/6.2011-3203`.

8. RESPONSIBILITY NOTICE

The following text, properly adapted to the number of authors, must be included in the last section of the paper: The author(s) is (are) the only responsible for the printed material included in this paper.